Electronic Supplementary Information

Solvent orientation in crystalline producing distinct magnetic dynamics in two binuclear Dy(III) polymorphs with polydentate Schiff base ligand

Zhijie Jiang, [‡a] Lin Sun,[‡a] Qi Yang,[a] Shilong Wei, [a] Hongshan Ke, [a] Sanping Chen,*[a] Yiquan Zhang,*[b] Qing Wei[a] and Gang Xie[a]

[a.] Key Laboratory of Synthetic and Natural Functional Molecule Chemistry of Ministry of Education, College of Chemistry and Materials Science, Northwest University, Xi'an, Shaanxi 710127, China.

[b.]Jiangsu Key Laboratory for NSLSCS, School of Physical Science and Technology, Nanjing Normal University, Nanjing 210023, China

Corresponding authors

Dr. Sanping Chen, Dr. Yi-Quan Zhang

E-mail address: sanpingchen@126.com; zhangyiquan@njnu.edu.cn

Table of Contents

1. General Remarks

All commercial reagents and solvents were purchased from Aldrich, Adamas and TCI. ^{1}H-and ^{13}C-NMR spectra were recorded on a Bruker AV-400 or AV-100 spectrometer. Chemical shifts (δ) were reported in parts per million (ppm) are referenced relative to the residual solvent peak in the NMR solvent ($CDCl_3$: δ 7.26 ($CHCl_3$)). ^{13}C chemical shifts were reported in parts per million are referenced to the carbon resonance of the solvent ($CDCl_3$: δ 77.16). Data are represented as follows: chemical shift, multiplicity (s =singlet, d = doublet, t = triplet, q = quartet, m = multiplet), integration, and coupling constants in Hertz (Hz). The FT-IR spectra were recorded in the range of 400-4000 cm^{-1} using KBr pellets on an EQUINOX55 FT-IR spectrophotometer. Elemental analysis (C, H, N) was implemented on a Perkin-Elmer 2400 CHN elemental analyzer. The phase purity of the bulk or polycrystalline samples was confirmed by powder X-ray diffraction (PXRD) measurements executed on a Rigaku RU200 diffractometer at 60 kV, 300 mA, and Cu Ka radiation (l = 1.5406 Å), with a scan speed of 51 min^{-1} and a step size of 0.02° in 2θ. Thermogravimetric analysis (TGA) were performed on a Mettler-Toledo TGA/DSC STARe thermal analyzer in the range of 25-600°C under a nitrogen flow at a heating rate of 5°C min^{-1}. Magnetic measurements were performed in the temperature range 2.0 K-300 K with an applied field of 1000 Oe, using a Quantum Design MPMS-XL-7 SQUID magnetometer on polycrystalline samples. The diamagnetic corrections for the complexes were estimated using Pascal's constants. Alternating current (ac) susceptibility experiments were performed using an oscillating ac field of 0 Oe at ac frequencies ranging from 1 to 1000 Hz. The magnetization was measured in the field range 0-70000 Oe.

2. X-ray crystallographic data

Table S1 Crystallographic data for complexes **1a** and **1b**.

Complexes	**1a**	**1b**
Empirical formula	$C_{56}H_{52}Cl_{10}Dy_2N_8O_6$	$C_{56}H_{52}Cl_{10}Dy_2N_8O_6$
Formula weight	1612.56	1612.56
Crystal system	Monoclinic	Monoclinic
Space group	$P2_1/c$	$C2/c$
a (Å)	12.8652(16)	21.186(9)

b (Å)	13.2912(18)	15.093(9)
c (Å)	21.1257(18)	21.803(12)
α(°)	90.00	90.00
β(°)	119.797(5)	116.915(14)
γ(°)	90.00	90.00
V (Å3)	3134.8(6)	6217(6)
Z	2	4
F (000)	1588	3176
$R1^{[a]}$, [I > 2*σ*(I)]	0.0401	0.0494
$wR_2^{[b]}$, [I > 2*σ*(I)]	0.0890	0.1162
$R1^{a}$, (all data)	0.0680	0.0760
wR_2^{b}, (all data)	0.1010	0.1261
GOF on F^2	0.967	1.094

$^{a}R_1 = \Sigma(F_o - F_c)/\Sigma F_o$. $^{b}wR_2 = [\Sigma w(F_o^2 - F_c^2)^2/\Sigma w(F_o^2)^2]^{1/2a}$.

Table S2 Selected bond lengths and angles for complexes **1a** and **1b**.

1a					
Dy(1)-O(3)	2.229(4)	O(2)-Dy(1)-O(1)^{i}	140.21(14)	O(2)-Dy(1)-N(1)	110.23(14)
Dy(1)-O(2)	2.234(4)	O(1)-Dy(1)-O(1)^{i}	69.21(15)	O(1)-Dy(1)-N(1)	72.11(13)
Dy(1)-O(1)	2.317(4)	O(3)-Dy(1)-N(2)	77.14(16)	O(1)^{i} -Dy(1)-N(1)	82.90(13)
Dy(1)-O(1)^{i}	2.330(3)	O(2)-Dy(1)-N(2)	71.45(15)	N(2)-Dy(1)-N(1)	66.43(15)
Dy(1)-N(2)	2.497(5)	O(1)-Dy(1)-N(2)	115.04(14)	N(4)-Dy(1)-N(1)	143.24(16)
Dy(1)-N(4)	2.498(5)	O(1)^{i} -Dy(1)-N(2)	144.08(15)	O(3)-Dy(1)-N(3)^{i}	111.17(14)
Dy(1)-N(1)	2.745(4)	O(3)-Dy(1)-N(4)	72.08(16)	O(2)-Dy(1)-N(3)^{i}	81.13(14)
Dy(1)-N(3)^{i}	2.774(4)	O(2)-Dy(1)-N(4)	78.31(15)	O(1)-Dy(1)-N(3)^{i}	82.46(12)
O(3)-Dy(1)-O(2)	138.51(14)	O(1)-Dy(1)-N(4)	143.52(15)	O(2)-Dy(1)-N(1)	110.23(14)
O(3)-Dy(1)-O(1)	139.98(13)	O(1)^{i} -Dy(1)-N(4)	113.98(14)	O(1)-Dy(1)-N(1)	72.11(13)
O(2)-Dy(1)-O(1)	79.21(14)	N(2)-Dy(1)-N(4)	84.15(16)	O(1)^{i} -Dy(1)-N(1)	82.90(13)
O(3)-Dy(1)-O(1)^{i}	79.56(14)	O(3)-Dy(1)-N(1)	79.94(14)	N(2)-Dy(1)-N(1)	66.43(15)
^{i} -x,-y,-z+1					
1b					
Dy(1)-O(3)	2.223(5)	O(1)-Dy(1)-O(2)	80.77(17)	O(2)^{i} -Dy(1)-N(2)	72.45(17)
Dy(1)-O(1)	2.240(5)	O(2)^{i} -Dy(1)-O(2)	69.42(18)	O(2)-Dy(1)-N(2)	84.08(16)
Dy(1)-O(2)^{i}	2.333(4)	O(3)-Dy(1)-N(3)	76.8(2)	N(3)-Dy(1)-N(2)	144.16(19)
Dy(1)-O(2)	2.338(5)	O(1)-Dy(1)-N(3)	71.8(2)	O(2)^{i} -Dy(1)-N(2)	72.45(17)
Dy(1)-N(3)	2.482(6)	O(2)^{i} -Dy(1)-N(3)	141.61(19)	O(2)-Dy(1)-N(2)	84.08(16)
Dy(1)-N(1)	2.494(6)	O(2)-Dy(1)-N(3)	114.53(18)	N(1)-Dy(1)-N(2)	66.14(18)
Dy(1)-N(2)	2.727(6)	O(3)-Dy(1)-N(1)	71.5(2)	O(3)-Dy(1)-N(4)	81.84(18)

Dy(1)-N(4)	2.792(6)	O(1)-Dy(1)-N(1)	76.7(2)	O(1)-Dy(1)-N(4)	110.26(19)
O(3)-Dy(1)-O(1)	137.15(19)	O(2)^{i} -Dy(1)-N(1)	115.58(17)	O(2)^{i} -Dy(1)-N(4)	81.33(16)
O(3)-Dy(1)-O(2)^{i}	78.77(17)	O(2)-Dy(1)-N(1)	144.57(19)	O(2)-Dy(1)-N(4)	70.07(16)
O(1)-Dy(1)-O(2)^{i}	142.24(17)	N(3)-Dy(1)-N(1)	83.8(2)	N(3)-Dy(1)-N(4)	66.27(19)
O(1)-Dy(1)-O(2)^{i}	142.24(17)	O(3)-Dy(1)-N(2)	109.32(18)	N(1)-Dy(1)-N(4)	143.87(18)
O(1)-Dy(1)-O(2)	80.77(17)	O(1)-Dy(1)-N(2)	82.14(18)	N(2)-Dy(1)-N(4)	148.35(17)
^{i} -x+1/2,-y+1/2,-z					

Table S3 The C (CH_2Cl_2) coordinates (x, y, z) in **1a** and **1b**.

	X	Y	Z
C (**1a** - CH_2Cl_2)	-2.420	6.518	10.560
C (**1b** - CH_2Cl_2)	-0.268	5.711	3.947

Table S4 The calculated results for Dy(III) ions configuration of complexes **1a** and **1b** by SHAPE 2.0 software.

Configuration	ABOXIY, **1a**	ABOXIY, **1b**
Hexagonal bipyramid (D_{6h})	15.989	16.113
Cube (O_h)	10.389	10.882
Square antiprism (D_{4d})	**1.321**	**1.356**
Triangulardodecahedron (D_{2d})	3.360	3.073
Johnson gyrobifastigium J26 (D_{2d})	17.523	17.344
Johnson elongated triangular bipyramid J14 (D_{3h})	25.650	26.131
Biaugmentedtrigonal prism J50 (C_{2v})	4.044	3.904
Biaugmentedtrigonal prism (C_{2v})	3.212	3.101
Snub siphenoid J84 (D_{2d})	6.391	6.355

3. The ^{1}H NMR and ^{13}C NMR spectra of H_3Clapi

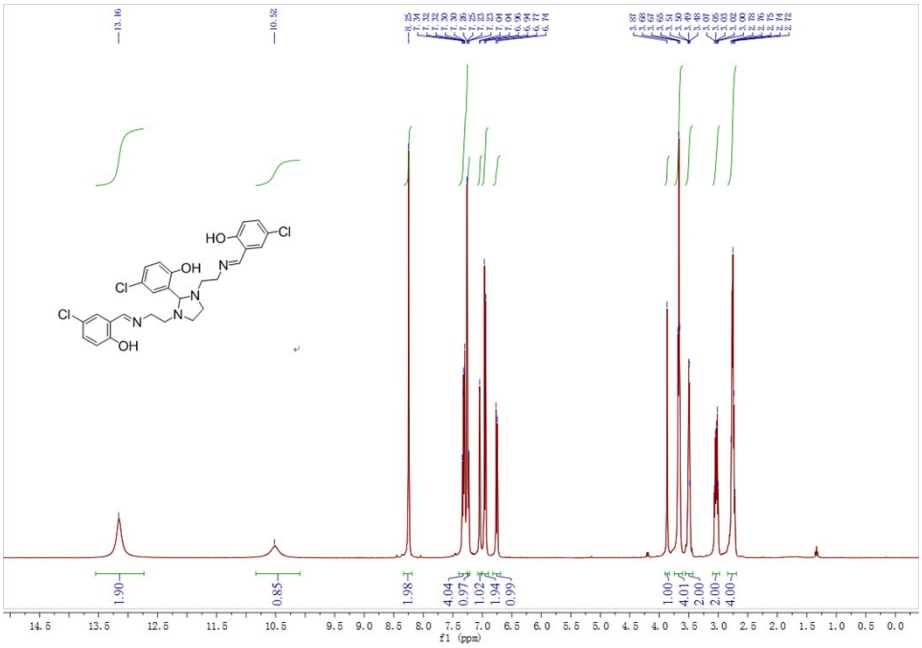

Fig. S1 ^{1}H-NMR spectra of H_3Clapi.

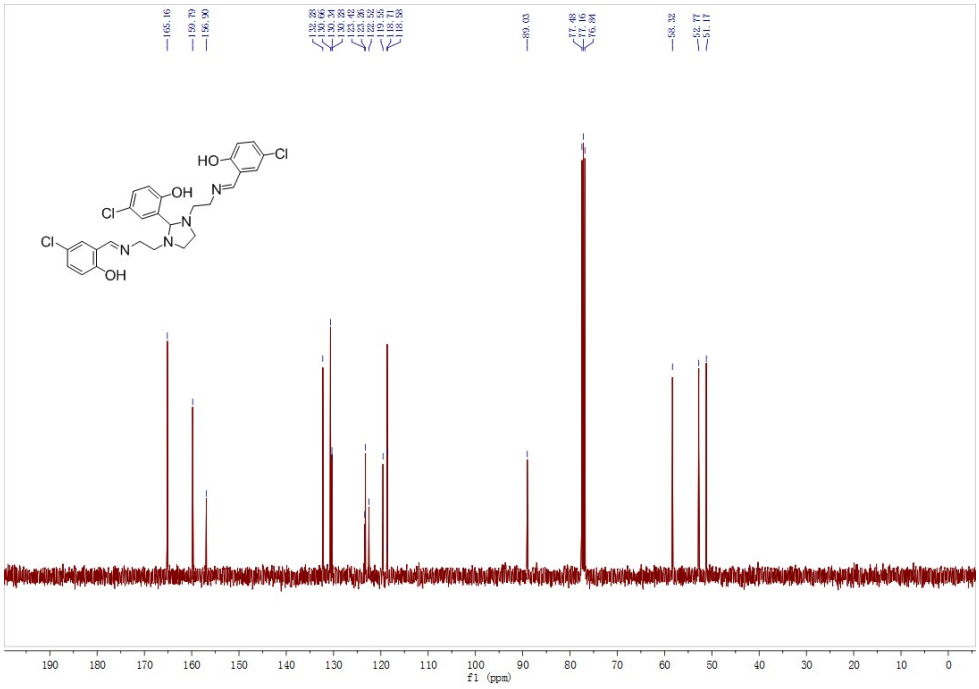

Fig. S2 ^{13}C-NMR spectra of H_3Clapi.

4. Thermogravimetric analysis

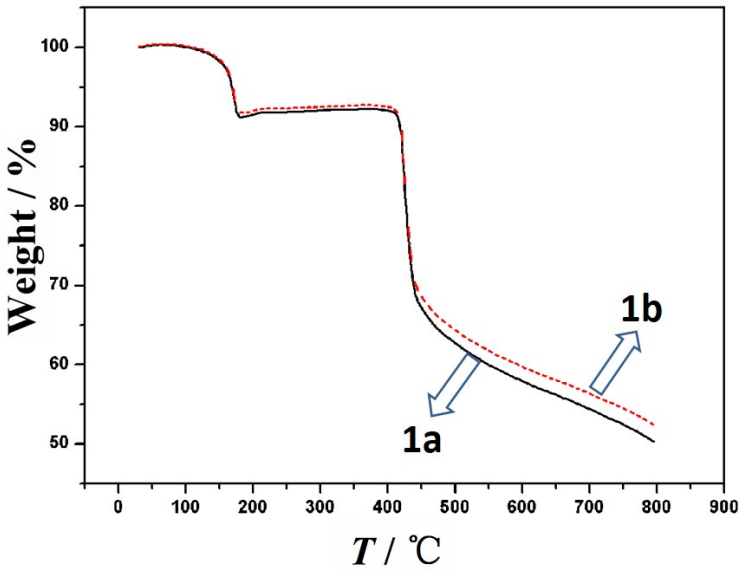

Fig. S3 TG curves for complexes **1a** and **1b**.

5. X-Ray Powder Diffraction

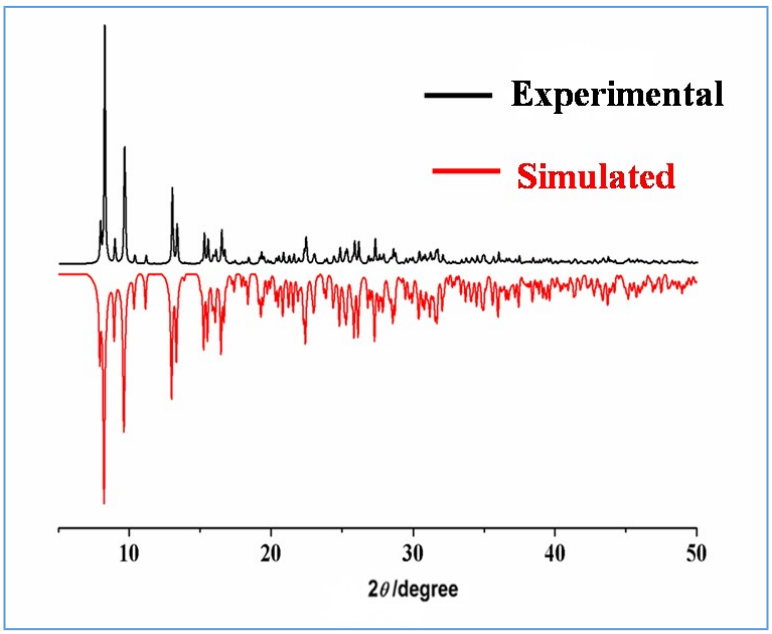

Fig. S4 Experimental and simulated PXRD of complex **1a**.

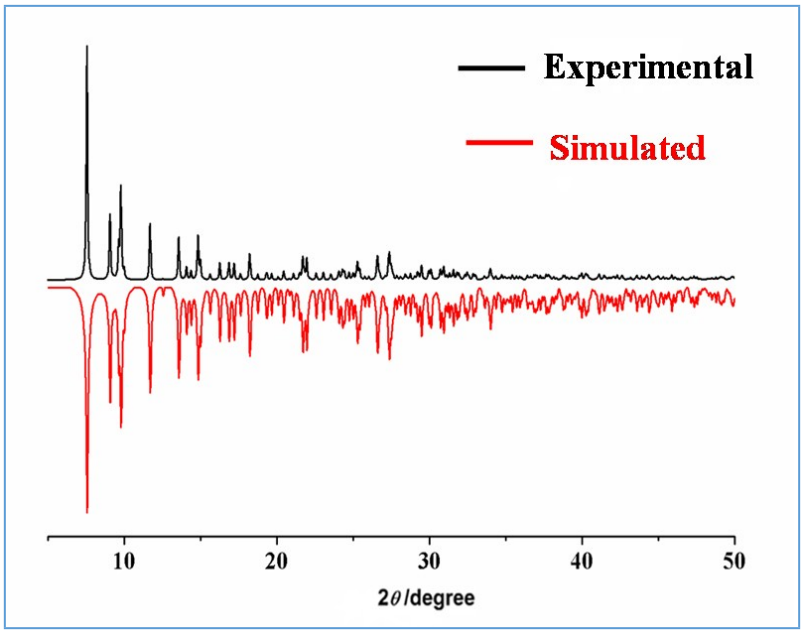

Fig. S5 Experimental and simulated PXRD of complex **1b**.

6. Crystal Structure

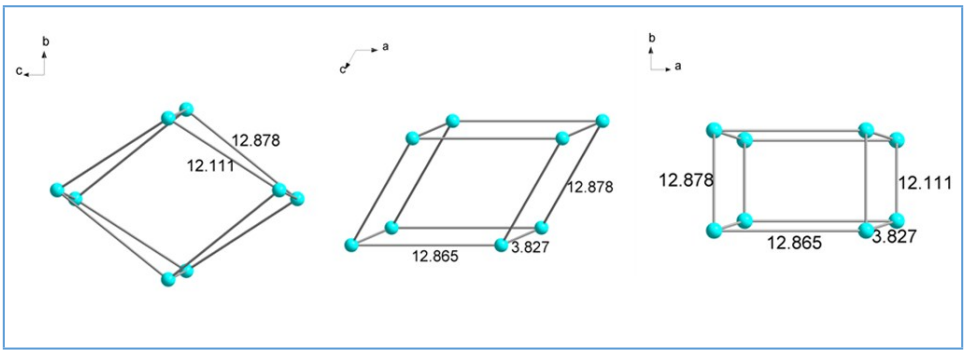

Fig. S6 The distances of dinuclear Dy units in complex **1a**, along the *a* axis, along the *b* axis, along the *c* axis.

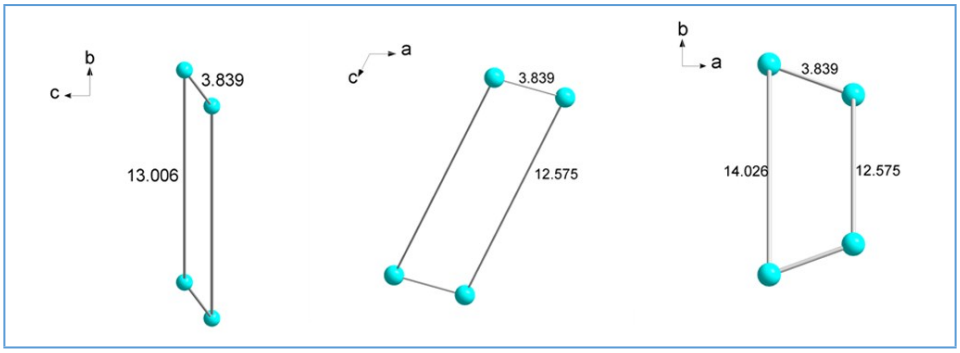

Fig. S7 The distances of dinuclear Dy units in complex **1b**, along the *a* axis, along the *b* axis, along the *c* axis.

7. Magnetic Measurements

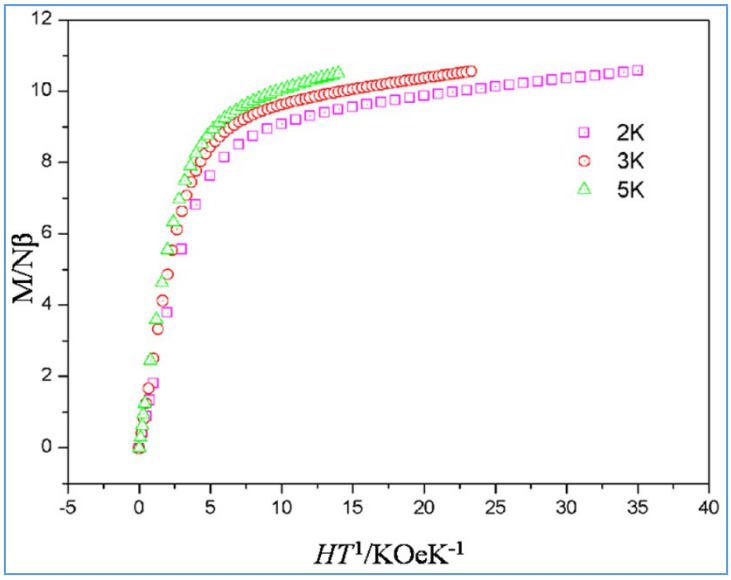

Fig. S8 Experimental *M* versus *H*/*T* plots of complex **1a** measured at 2.0 K, 3.0 K and 5.0 K

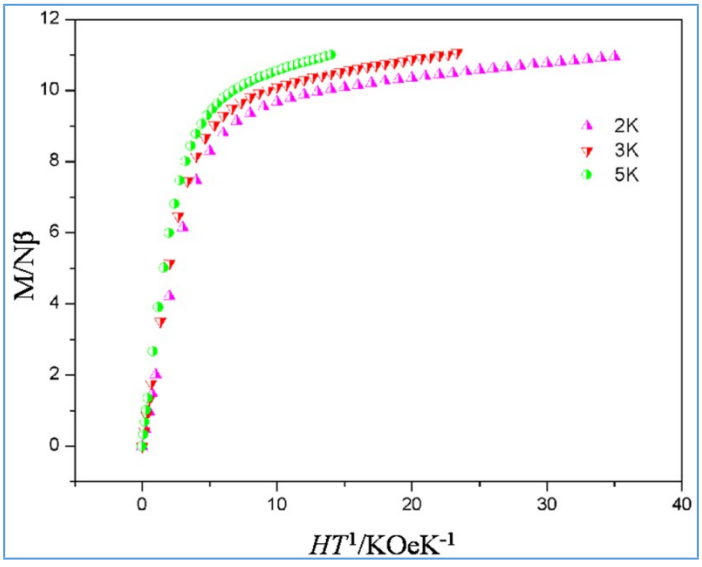

Fig. S9 Experimental *M* versus *H*/*T* plots of complex **1b** measured at 2.0 K, 3.0 K and 5.0 K

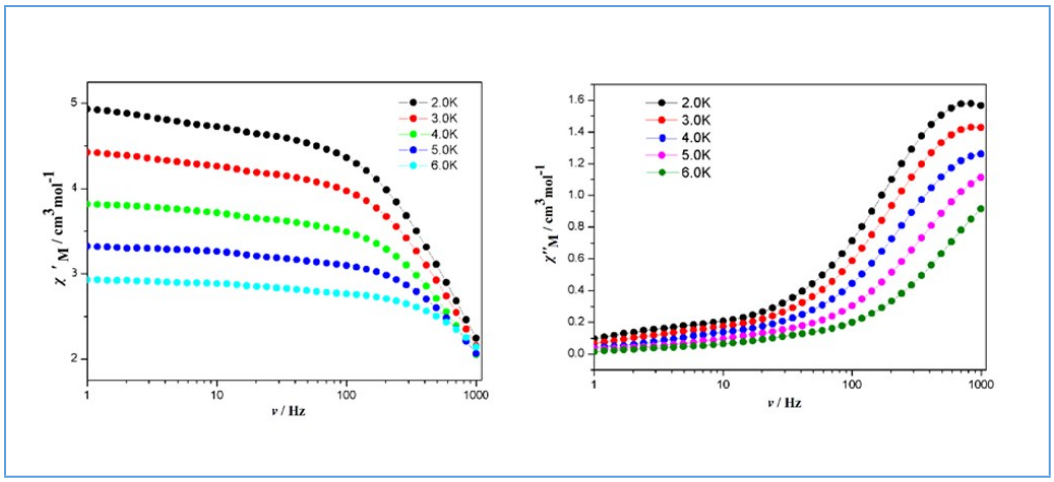

Fig. S10 Frequency dependent in-phase (χ M ') and out-of-phase (χ M '') signals for complex **1a** at zero dc field.

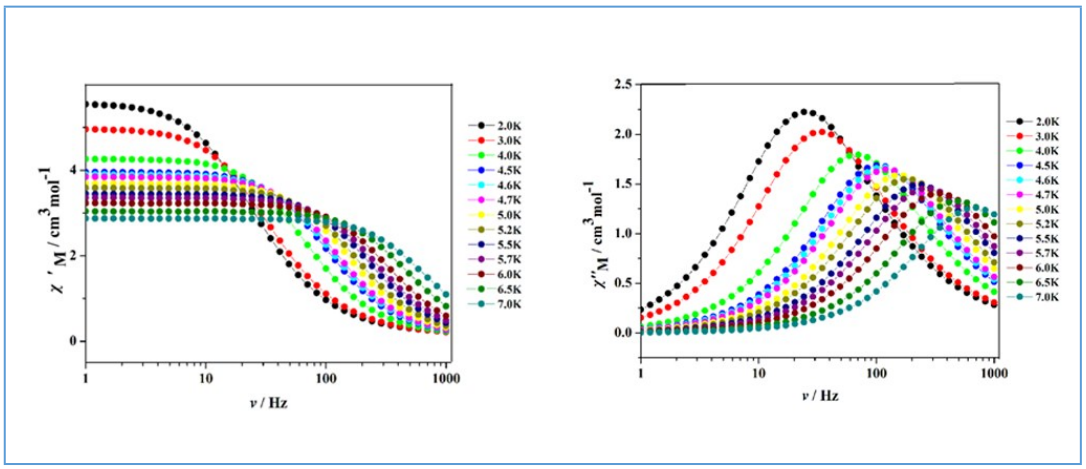

Fig. S11 Frequency dependent in-phase (χ M ') and out-of-phase (χ M '') signals for complex **1b** at zero dc field.

8. Theoretical investigation of the Polymorphs

Study of the Relative Stability of the Polymorphs. We started the computational study by computing the relative energy of the both polymorphs using the crystallographic coordinates as starting points for the optimization in the gas phase. It can be observed that the energetic difference between complexes **1a** and **1b** is negligible at 0.29 kcal·mol^{-1}. It should be mentioned that both structures (minima) are found on the potential hypersurface, which agrees with the experimental observation of polymorphs **1a** and **1b**.

9. Computational details

Complete-active-space self-consistent field (CASSCF) calculations on individual lanthanide Dy(III) fragment of the complete structures (see Fig. S14 for the complete structure of complex **1a**) on the basis of single-crystal X-ray determined geometry has been carried out with MOLCAS 8.0 program package. The dinuclear complexes **1a** and **1b** have an inversion center, and thus we only need to calculate one magnetic center. During the calculation, the other Dy(III) ion was replaced by diamagnetic Lu(III). The basis sets for all atoms are atomic natural orbitals from the MOLCAS ANO-RCC library: ANO-RCC-VTZP for Dy(III) ions; VTZ for close O and N; VDZ for distant atoms. The calculations employed the second order Douglas-Kroll-Hess Hamiltonian, where scalar relativistic contractions were taken into account in the basis set and the spin-orbit couplings were handled separately in the restricted active space state interaction (RASSI-SO) procedure. For the fragment of individual Dy(III) ion, active electrons in 7 active spaces include all *f* electrons (CAS (9 in 7)) in the CASSCF calculation. To exclude all the doubts, we calculated all the roots in the active space. We have mixed the maximum number of spin-free state which was possible with our hardware (all from 21 sextets, 128 from 224 quadruplets, 130 from 490 doublets for the Dy(III) fragment).

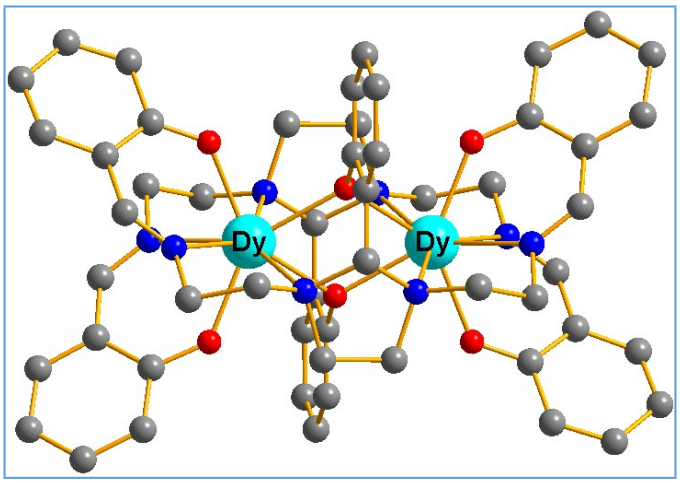

Fig. S12 Calculated complete structure of complex **1a**; H atoms are omitted.

To fit the exchange interaction in both complexes, we took two steps to obtain them. Firstly, we calculated one Dy(III) fragment using CASSCF to obtain the corresponding magnetic properties. And then, the exchange interaction between the magnetic centers is considered within the Lines model,[2] while the dipole-dipole magnetic coupling is treated exactly. The Lines model is effective

and has been successfully used widely in the research field of f-element single-molecule magnets.[3]

For complexes **1a** and **1b**, there is only one type of *J*.

The exchange Hamiltonian is:

$$\hat{H}_{exch} = -J_{total}\,\hat{S}_{Dy1}\,\hat{S}_{Dy1'} \qquad \text{(S1)}$$

The J_{total} is the parameter of the total magnetic interaction ($J_{total} = J_{diploar} + J_{exchange}$) between magnetic center ions. The $\hat{S}_{Dy} = \pm 1/2$ are the ground pseudospin on the Dy(III) sites. The dipolar magnetic coupling can be calculated exactly, while the exchange coupling constants were fitted through comparison of the computed and measured magnetic susceptibility using the POLY_ANISO program.[4] We also gave the exchange energies and the main values of the g_z for the lowest two exchange doublets of complexes **1a** and **1b** in Table S4 and S5 where the g_z values of the ground exchange state for complexes **1a** and **1b** are both close to 0, which confirms that the Dy(III)-Dy(III) coupling are all antiferromagnetic.

Table S4 Exchange energies (cm^{-1}) and main values of the g_z for the lowest two exchange doublets of complexes **1a** and **1b**.

	1a		**1b**	
	E	g_z	*E*	g_z
1	0.0	0.000	0.0	0.000
2	1.5	37.156	1.8	36.998

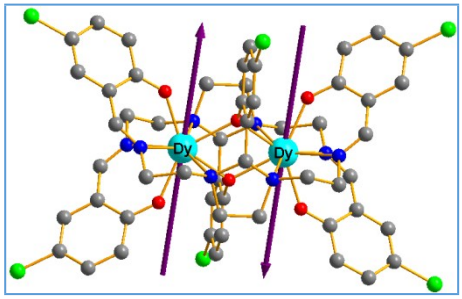

1a

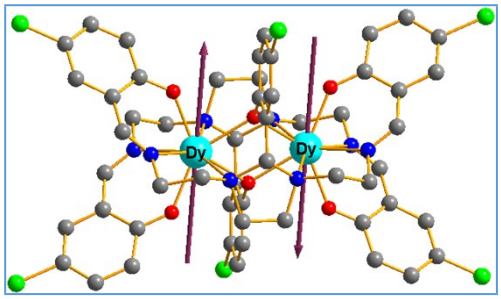

1b

Fig. S13 Orientations of the local main magnetic axes of the ground doublets on Dy(III) ion of complexes **1a** and **1b**.

10. References

(1). G. Karlström, R. Lindh, P.-Å. Malmqvist, B. O. Roos, U. Ryde, V. Veryazov, P.-O. Widmark, M. Cossi, B. Schimmelpfennig, P. Neogrady and L. Seijo, *Comput. Mater. Sci.*, 2003, **28**, 222-239.

(2). M. E. Lines, *J. Chem. Phys*., 1971, **55**, 2977-2984.

(3). (a) K. C. Mondal, A. Sundt, Y. Lan, G. E. Kostakis, O. Waldmann, L. Ungur, L. F. Chibotaru, C. E. Anson and A. K. Powell, *Angew. Chem. Int. Ed.*, 2012, **51**, 7550-7554. (b) S. K. Langley, D. P. Wielechowski, V. Vieru, N. F. Chilton, B. Moubaraki, B. F. Abrahams, L. F. Chibotaru and K. S. Murray, *Angew. Chem. Int. Ed*., 2013, **52**, 12014-12019.

(4). (a) L. F. Chibotaru, L. Ungur and A. Soncini, *Angew. Chem. Int. Ed*., 2008, **47**, 1224-1230. (b) L. Ungur, W. Van den Heuvel and L. F. Chibotaru, *New J. Chem*., 2009, **33**, 4126-4129. (c) L. F. Chibotaru, L. Ungur, C. Aronica, H. Elmoll, G. Pilet and D. Luneau, *J. Am. Chem. Soc*., 2008, **130**,12445-12455.